NPL REPORT COAM 17

Towards an improved determination of the Avogadro constant

by
Richard Brown and Martin Milton

January 2003

Towards an improved determination of the Avogadro constant

by
Richard Brown and Martin Milton

ISSN 1475-6684

National Physical Laboratory
Queens Road, Teddington, Middlesex, TW1 0LW

Approved on behalf of Managing Director, NPL
By D H Nettleton, Head of the Centre for Optical and Analytical Measurement

Executive summary

The Avogadro constant (N_A) is the fundamental constant that relates quantities at the atomic scale to those at the macroscopic scale. It is currently of particular interest because an experimental determination of the Avogadro constant is one of several possible ways to re-define the kilogram ultimately leading to a replacement of the prototype kilogram at BIPM. In order to do this N_A must be determined with a relative uncertainty of 1 part in 10^8. This report presents an introduction to the measurement of N_A, a review of the XRCD technique currently used for its determination and some of the difficulties associated with it. The report goes on to propose some alternative experimental methods based on ion accumulation exploiting new technologies and novel mass artefacts, and comments on how each may contribute to improved determinations of the Avogadro constant. They deserve further investigation as technologies improve.

Table of Contents

Executive summary 2
Table of Contents 3
1. Introduction 4
2. History and progress in the measurement of N_A 6
2.1 The Avogadro (N_A) and Faraday (F) constants 6
2.2 XRCD and The International Working Group on the Avogadro Constant 8
2.3 Limiting uncertainties in the method 9
3. Alternative methods for the determination of N_A 13
3.1 Indirect determinations of N_A from other fundamental constants 13
3.2 Ion accumulation 15
4 New artefacts and materials 16
4.1 Clusters and Fullerenes 16
4.2 Macromolecules 20
4.3 Biological structures 23
5. New technologies for N_A measurement with large molecules 27
5.1 High current ion guns 27
5.2 Ion-cyclotron resonance mass spectrometry 28
5.3 SQUID ion current detectors 28
5.4 Improving collection efficiency 29
6. Summary 32
7. Acknowledgements 32
8. References 33

1. Introduction

The quantity 'amount of substance' is required to provide a coherent basis for dimensional analysis within chemistry [1]. The assigned unit for amount of substance, the mole, was introduced as a base quantity of the SI in 1971. It is defined as, "The amount of substance of a system which contains as many elementary entities as there are atoms in 0.012 kg of ^{12}C. When the mole is used, the elementary entities must be specified and may be, atoms, molecules, ions, electrons, or other particles or specified groups of particles" [2]. The existence of the mole amongst the base units of the SI enables the results of measurements of amounts of substance to be expressed unambiguously. For example, the quantity amount ratio expressed in terms of mol/mol, can be clearly distinguished from mass ratio expressed in terms of kg/kg.

The constant which relates quantities at the microscopic scale to those at macroscopic scale is the Avogadro constant, N_A. One mole of any substance contains Avogadro's number of elementary particles. Whether a mole of atoms, a mole of molecules, a mole of electrons, or a mole of ions is under consideration, by definition, a mole always contains N_A of the elementary particles involved. The mass of a mole of any species is simply the relative atomic, molecular or ionic mass of the species in grams. The Avogadro constant, also known as Avogadro's number, forms the numerical link between the most basic quantity in chemistry, amount of substance, and the most basic quantity in physics, mass. It permits calculation of the amount of pure substance and is the basis of stoichiometric relationships. It also makes possible the determination of the mass of a simple molecule of one gas relative to that of another, and as a result the relative molecular weights of gases can be ascertained by comparing the weights of equal volumes via Dalton's law of partial pressures.

Inspired by an observation by Joseph Gay-Lussac (1778-1850), Lorenzo Romano Amadeo Carlo Avogadro (1776-1856) proposed his hypothesis in 1811, that the number of molecules in a given volume of gas at a given temperature is the same for all gases regardless of their chemical nature or physical properties. As he was unable to prove his proposal, the statement became known as Avogadro's Hypothesis, and the determination of this constant has fascinated scientists ever since.

The earliest determination of N_A by Loschmidt in 1865 was $72(1) \times 10^{23}$ mol^{-1}, based on estimates of molecular diameters and mean free path lengths. Progress in the determination of N_A since 1865, and its relative uncertainty, is charted in Figure 1. The relative uncertainty of the quoted value has decreased by approximately an order of magnitude over every 20 years since 1920 leading to the currently accepted value of $6.022\ 141\ 99(47) \times 10^{23}$ mol^{-1} [3], determined using X-ray/crystal density measurements.

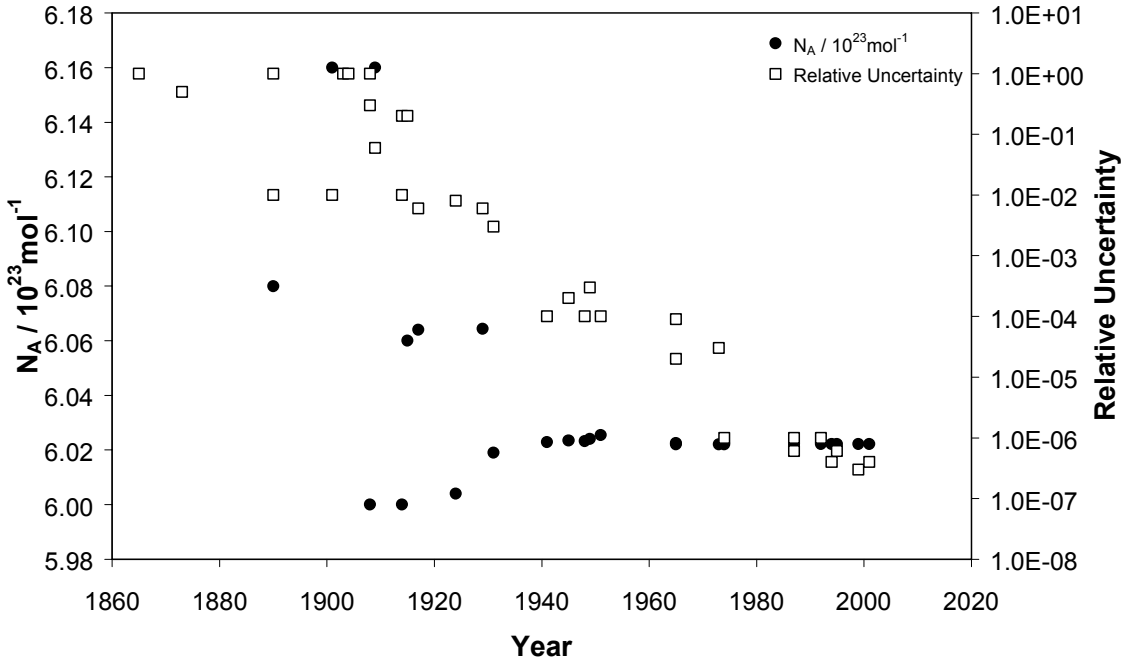

Figure 1 Progress in the determination of N_A since 1865, together with the relative uncertainty (from data in reference 4). Values of N_A not shown: 72 (1865), 11 (1873), 7 (1890), 9.3 (1903), 8.7 (1904), 6.7 (1908), 5.91 (1914) and 5.9 (1923). Before 1924, data was derived mainly from atomic or molecular movement in gases or fluids. Between 1929 and 1951 it was mainly from X-ray wavelengths and data from 1965 until the present day mainly from X-ray/crystal density measurements [4].

In the last 10 years, there has been a great deal of interest in the accurate determination of N_A as a possible basis for a re-definition of the kilogram. The unit of mass is the only base unit that is realised artefactually, by the prototype kilogram. A re-definition would be a major step forward for metrology since the prototype kilogram, manufactured from a platinum-iridium alloy, exhibits long term instability. (The instability has been estimated to be $\Delta m / m \approx 5x10^{-8}$ over the past 100 years [5]).

The aim of such experiments to determine the Avogadro constant is to arrive at a n experimental redefinition of the unit of mass in terms of atomic masses. The use of the Avogadro constant in this way requires a final relative measurement uncertainty of 1 x 10^{-8}. Extrapolation from Figure 1 suggests that this level of precision may not be reached until 2025. The exploration of alternative experimental methodologies is therefore advisable to improve the chance of a replacement of the kilogram artefact within the next thirty years.

2. History and progress in the measurement of N_A

The earliest estimates of N_A were made using kinetic gas theory via the estimation of molecular diameters and mean free paths and additionally from observations of Brownian motion. The characteristic thermal motion of molecules can also be observed in liquids. However since the number density of molecules in a liquid is 1000 times greater than in a gas, the mean free paths are dramatically smaller and inter-molecular effects can no longer be ignored. In 1890 Rayleigh and Rőntgen investigated thin molecular films on water and obtained values for molecular diameters leading to values for the number of particles in a mole. An improved analysis by DuNout in 1924 obtained a value of 6.003×10^{23} mol^{-1} for N_A. One of the final attempts to derive a value for the Avogadro constant by observing particle motion was by Kappler in 1931, who observed the Brownian motion of a torsion balance, which led to a value of 6.059×10^{23} mol^{-1}.

After the discovery of radioactivity, determinations of N_A were published by Rutherford (1909) and Gleditsch (1919) based on the production of helium from radium, and the half-life period of radium, respectively. However the method of choice for determination of the Avogadro soon became based on X-ray crystallography.

In 1900 the electromagnetic nature of X-rays was postulated and the driving force behind the next 100 years of N_A determination was established. In 1914 Bragg used published values of the Avogadro constant to determine the lattice parameter of NaCl crystals. Subsequently this experiment was reversed in order to calculate values for N_A using X-rays. The determination of the Avogadro constant using X-rays also required the mean molar mass and the macroscopic density of the target crystal, usually carried out by hydrostatic weighing. Most of the early work in this area used calcite crystal, although diamond, LiF and KCl were also used. (Single crystals of copper have been used for low-precision N_A determinations [6]). These methods yielded results less than 2 parts in 10^5 away from today's accepted value. The advent of the use of Silicon (Si) in the 1960s, a material with fewer lattice defects and better quality, together with more highly defined X-ray sources has advanced the science of N_A measurement to its current level.

2.1 The Avogadro (N_A) and Faraday (F) constants

The Faraday constant, F, is the charge required to deposit one mole of a substance on an electrode during electrolysis. Hence, the Avogadro and Faraday constants are related by the electron charge (e):

$$F = N_A e \tag{1}$$

An experimental determination of the Faraday constant via electrolysis using a coulometer requires the measurement of the time integral of a current, so that the charge transferred (q) can be determined from $q = I\Delta t$.

Solution-based electrochemical techniques for the determination of N_A have never been developed to the highest possible precision. They are usually limited to laboratory demonstrations or low precision determinations [7]. However the basis of solution electrochemical determinations is experimentally sound. Dynamic solution electrochemistry remains a valid and potentially useful means for evaluating N_A but the technique requires a thorough metrological treatment. It usually involves one of two electrolytic processes, the oxidative dissolution of copper from a copper anode in sulphuric acid (Equation 2a) or the reduction of the sulphuric acid itself (Equation 2b):

$$Cu \rightarrow Cu^{2+} + 2e^{-} \quad (2a)$$

$$2H^{+} + 2e^{-} \rightarrow H_2 \quad (2b)$$

The total charge passed during the chosen electrolysis reaction is measured and the mass loss from the copper or the volume gain of hydrogen is determined and converted into an amount. N_A is then given from a determination of the Faraday constant:

$$Q = nF = neN_A \quad (3)$$

where Q is the total charge passed, n is the amount of copper or hydrogen produced, F is the Faraday constant and e is the electronic charge.

In 1980, an Ag coulometer was used at NIST to determine F and therefore indirectly N_A [8,9]. In the experiments the amount of silver dissolved was either approximately 3 or 5g and the current used was either 100 or 200mA, with the duration of the runs being between 3 and 12 hours. One of the major contributors to the estimated uncertainty of 133×10^{-8} was the measurement of the amount of silver lost non-electrolytically from the anode. In view of the difficulty of confirming the efficiency of the chemical reaction upon which the silver dissolution coulometer is based and the effects of impurities in the silver, it was thought unlikely that the uncertainty of this type of experiment could be significantly reduced.

Another potential route for solution-based electrochemical determinations is to reverse the electrolytic process and examine the electrochemical deposition of much more massive entities, such as those discussed in Section 4. Providing that the electrochemical conditioning was such that the deposited species were uniformally packed on the substrate/electrode surface with no intercalation of supporting electrolyte or impurities, such a method should be able to achieve higher levels of precision than are currently possible using electrolytic processes.

2.2 XRCD and The International Working Group on the Avogadro Constant

Current experimental determinations of the Avogadro constant are based on the XRCD method, which combines the results of X-ray/optical interferometry of the lattice period with measurements of the macroscopic density (crystal density) and isotopic abundance ratios of a highly pure Si sample.

The XRCD technique is based on the equality of the molar volume determined by the microscopic (left hand side of equation 4) and macroscopic (right hand side of equation 4) scales:

$$\frac{N_A}{\upsilon} a_0^3 = \frac{M}{\rho} \tag{4}$$

Where ρ is the density of the macroscopic silicon artefact with a known RMM, a_0^3 is the cell volume and υ is the number of atoms in the unit cell. This leads to an expression for N_A in terms of the mass content of a perfect unit cell.

$$N_A = \frac{nM}{\rho a_0^3} \tag{5}$$

Where M is the mean molar mass of the atoms.

The earliest determinations of N_A using a XRCD method were by Birge [10] and Straumanis [11] in the 1940s. The first realization of N_A by an International Working Group on the Avogadro Constant was at the NBS (now NIST) in the mid-seventies. Work by other NMIs, particularly PTB, subsequently exposed a significant error in the NBS work. Even by the early 1990s, the levels of realized precision were significantly below what is required for a redefinition of the unit of mass. These external and internal difficulties led to the formation of a new working group to review the situation and provide recommendations as to the future course of such measurement technologies.

The present Avogadro Group [12] began as an *ad hoc* group under the auspices of the Comité Consultatif pour la Masse et le grandeurs apparentees (CCM). A detailed rationale for this working group was given as follows:

> "A more accurate value of the Avogadro constant N_A will be a key input parameter to tabulated values of the fundamental constants. Current efforts to re-determine this constant by evaluating physical and chemical properties of single-crystal silicon rely heavily on primary standards of length, mass and amount of substance, and thus provide challenges in several areas of metrology. Measurements carried out with a view to obtaining a more accurate value of N_A based on silicon have been undertaken by a variety of metrological and chemical laboratories including, of course, your own.
>
> The main reasons for forming an *ad hoc* Working Group and for placing it within the CCM are:

1. A new determination of N_A requires accurate measurements and a theoretical understanding of key silicon properties such as lattice spacing, density, molar mass etc., which are the subjects of independent study in a number of laboratories. Efficiency can be improved through regular exchanges of information and, perhaps, other forms of cooperation.
2. Laboratories with competence in the key areas are generally in metrology institutes. The establishment of a Working Group within the CCM confirms that such work is part of an international effort of great metrological interest.
3. A more accurate value for N_A, the conversion factor between microscopic and macroscopic amounts of matter, would set improved limits on the stability of the present standard of mass and may help in the long-term program to re-define the kilogram."

2.3 Limiting uncertainties in the method

As can be seen from equation 4, N_A is simply the ratio of the molar volume V_{mol} to the atomic volume V_{at} or equally the ratio of the molar mass M_{mol} to the atomic mass m_{at}.

$$N_A = \frac{V_{mol}}{V_{at}} = \frac{M_{mol}}{m_{at}} \tag{6}$$

In order to perform this calculation several quantities must be measured on the same Si crystal. The Si artefacts are very high purity boules (with a diameter of approximately 10 cm), similar to the one shown in Figure 2, that are grown using the Float Zone process. They are nitrogen doped to reduce the content of swirl defects. The quantities measured are:

- The volume occupied by a single Si atom. This is derived from knowledge of the structure and lattice spacing of a highly perfect, highly pure silicon crystal. (These measurements also include precise investigations into the content of impurity atoms and self-point crystal defects). The spacing between the (220) lattice planes is determined using a scanning X-ray interferometer. This value can be converted to give the unit cell volume. The separation between these planes is approximately 0.192 nm.

- The macroscopic density. The Si artefact is placed within an etalon and its diameter is measured using optical interferometry. Many diameters can be measured and an average value determined, leading to a calculation of the volume.

- The isotopic composition and hence the molar mass. Silicon exists as three stable isotopes: ^{28}Si, ^{29}Si and ^{30}Si. Molar mass is determined by fluorinating the Si and measuring the isotope ration between the resulting SiF_4^+ ions with a precision Mass Spectrometer. The molar masses of each isotope (^{28}Si, ^{29}Si and ^{30}Si) are known with a relative uncertainty of less than 1 part in 10^8. Thus, the measurement of the molar mass of naturally occurring silicon relies on determining the isotopic ratios.

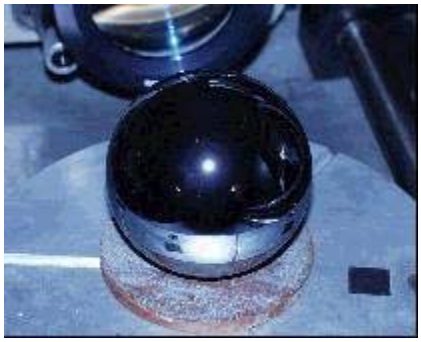

Figure 2 A high purity silicon boule (from reference 13).

An example of the uncertainties required to attain a total relative uncertainty of 1 x 10^{-8} for determination of N_A by XRCD methods are shown in Table 1.

Parameter	***Uncertainty***	***Effect on N_A (parts in 10^8)***
Molar Mass	0.1 μg.mol^{-1}	0.36
Mass	4 μg	0.40
Diameter	0.11 nm	0.33
Temperature	0.08 mK	0.36
Oxide Layer	<0.1 nm	0.56
Lattice parameter	0.2 x 10^{-3} fm	0.31
Atoms / unit cell	2 x 10^{-8}	0.25
Total		1.00

Table 1 An example of the component uncertainties required to reach a total uncertainty of 1 x 10^{-8} for a determination of the Avogadro constant.

There are several outstanding issues with the XRCD method that currently make the target uncertainty unattainable. These are discussed briefly below:

The counting of silicon atoms by XRCD presupposes knowledge of the number and type of impurities within the silicon (ideally zero) and their influence on the mass and volume. This consideration additionally includes the presence of lattice defects within the pure silicon itself. The following defects must be considered:

- Impurity atoms occurring on regular lattice sites by the substitution of silicon atoms.
- Impurities on interstitial sites, which increase the average number of atoms per unit cell.
- Si vacancies and Si self-interstitials favoured by the relatively small packing density of the lattice.

The absence of a definitive characterisation of the composition of the silicon artefacts is one factor which prevents the target uncertainty being attained. The growth conditions for the Si artefacts, normally chemical vapour deposition (CVD), have a great influence on the incorporated impurities. Carbon, oxygen, nitrogen (often deliberately used as a doping agent to prevent the agglomeration of self-point defects), hydrogen and more recently argon [14] in particular are noted as common lattice impurities within Si artefacts.

Additionally, a detailed knowledge of the isotopic composition of each Si artefact is required along with the effect of composition on physical properties in order to approach the target measurement uncertainties. The effect of isotopic composition (which may vary by more than 3 x 10^{-6} between crystals) has recently been investigated [15]. Isotopically enriched single crystals can provide artefacts with more consistent and well-defined lattice parameters. Up to a resolution of several femtometers the purity of semiconductor-grade silicon is high enough so that no correction need be made for imperfections. Once the femtometer boundary is crossed the actual content of impurity atoms, self-point defects and isotopic composition must be taken into account [4].

Absolute measurements of the silicon molar mass also require a precise measurement of the isotopic abundances within the Si artefact. The molar mass of the Si artefact $M(Si)$ may be expressed in terms of the molar mass of one of the stable isotopes thus:

$$M(Si) = M(^{28}Si)[1+\xi] \tag{7}$$

Where the fraction ξ must be measured with an uncertainty of 1 x 10^{-8}. Currently this measurement is extremely difficult and requires the conversion of single crystals to the gaseous compound SiF_4 whose isotopic distribution is then measured by an isotope-ratio gas mass spectrometer [16].

Despite accurate growth and production of the Si artefact, it is still likely to contain very thin amorphous silicon, silicon dioxide and contaminant layers on or near the surface that will affect the measurement of the macroscopic density. This is represented diagrammatically in Figure 3.

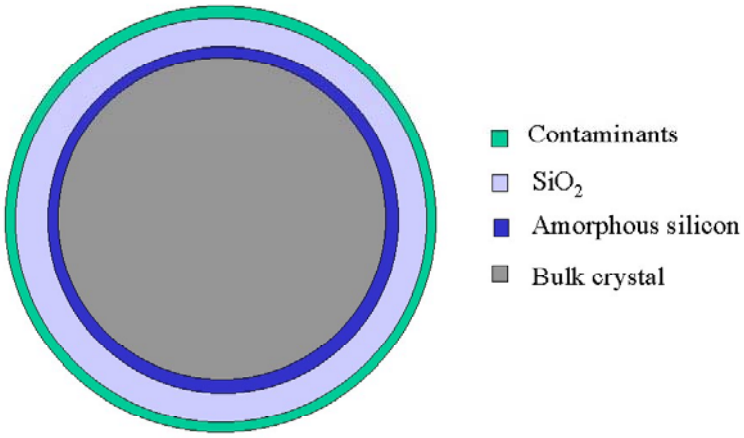

Figure 3 Representation of the cross-sectional composition of a Si artefact [not to scale] (from reference 13).

Corrections have to be applied to the measured bulk density of a sphere to take account of the presence of surface oxidation and possible contaminants (water, hydrocarbons etc). The density of the oxide is less than that of silicon. Furthermore, when determining the diameter interferometrically, the presence of an oxide leads to an apparent displacement of the surface. Ideally, the oxide should be of a uniform thickness, stable, with a well-defined composition and thin. If these conditions are not met treatment will be required.

A range of complementary techniques (ellipsometry, XPS, RBS, TEM and AFM) are also commonly used to characterise fully and monitor the stability of native oxides. Ultimately, the oxide thickness has to be determined with an uncertainty of less than 0.3 nm. The use of a chemical etch to remove the native oxide and any amorphous silicon present, and the subsequent growth of an ultra thin thermal oxide is currently being investigated [13].

Despite internationally agreed procedures, values for N_A determined at several locations around the world do not approach the ultimate relative uncertainty of 1×10^{-8} required to redefine the kilogram. The measurement uncertainty is primarily limited by problems associated with the preparation and characterisation of the Si artefact.

3. Alternative methods for the determination of N_A

3.1 Indirect determinations of N_A from other fundamental constants

It is possible to determine the Avogadro constant using indirect methods based on mathematical relationships between the fundamental physical constants. An indirect value for the Avogadro constant would be based primarily on the determination of the Rydberg constant R_∞, the fine structure constant ∞, and Planck's constant h [17]. A suitable method for calculating indirect values of N_A, from the molar Plank constant, $N_A h$, is from an expression for the Rydberg constant R_∞:

$$R_\infty = m_e c\alpha^2 / 2h = \frac{M_p c\alpha^2}{2(m_p / m_e)N_A h} \tag{8}$$

Where M_p is the proton molar mass, m_p is the proton mass, m_e is the electron mass and c is the velocity of electromagnetic radiation. In this determination the uncertainty in N_A is linked to the uncertainty in h. Equation (4) may be re-written as follows:

$$N_A = \frac{\mu_0 c^2 M_p \alpha (2e/h)^2}{16 R_\infty (m_p / m_e)} \tag{9}$$

Where μ_0 is the permeability of vacuum and e is the elementary charge. There are a number of ways of determining h, $2e/h$ (the Josephson constant, K_J) or h/e^2 (the quantum Hall resistance, R_K) most of which depend on the Josephson or quantum Hall effects. In 1990 conventional (exact) values of the Josephson constant and the quantum Hall resistance were adopted, K_{J-90} and R_{K-90} respectively. From this the Avogadro constant can be derived, based on the international realizations of the ohm and the volt:

$$N_A = \frac{M_p c\alpha^2 K_{J-90}^2 R_{K-90}}{32 R_\infty (m_p / m_e)} \tag{10}$$

Additionally using the adopted values for the Josephson constant and the quantum Hall resistance a value for N_A may be derived by determination of the Faraday constant F if one has an independent value for e:

$$N_A = \tfrac{1}{2} R_K K_J F \tag{11}$$

Alternatively, using the relationship between N_A and the Josephson constant and the quantum Hall resistance, a value for Avogadro's constant may be derived indirectly by measurement of h:

$$h = \frac{4}{K_J^2 R_K} \tag{12}$$

This has been done successfully at NPL and NIST using a Watt balance. The principle is understood by considering an electrical conductor carrying a current in a magnetic flux density. The force of the conductor can be measured by balancing it against the gravitational force acting on a mass. The experimental determination is then carried out in two steps. Firstly the gravitational force compensates the attracting electro-magnetic force between two coils. Secondly the coils are moved with respect to one another with constant velocity causing an induced voltage. h may then be derived from these measured parameters.

Determinations of h have also been successfully made by measurement quantity $\hbar / m$, in the case of neutrons diffracted from a silicon crystal, to a precision of 8 x 10^{-7}.

The values of N_A indirectly determined from the measurements of other constants with relative uncertainties, including the proton gyromagnetic ratio γ_p, are compared against the XRCD method in Figure 4. The CODATA values are based of new determinations of several important physical constants.

None of the values in Figure 4 manage to demonstrate a relative uncertainty better than 1 x 10^{-8}. The most precise determinations ascribe relative uncertainties of 8 x 10^{-8}, but these values are not consistent with the other determined values within the quoted measurement uncertainties.

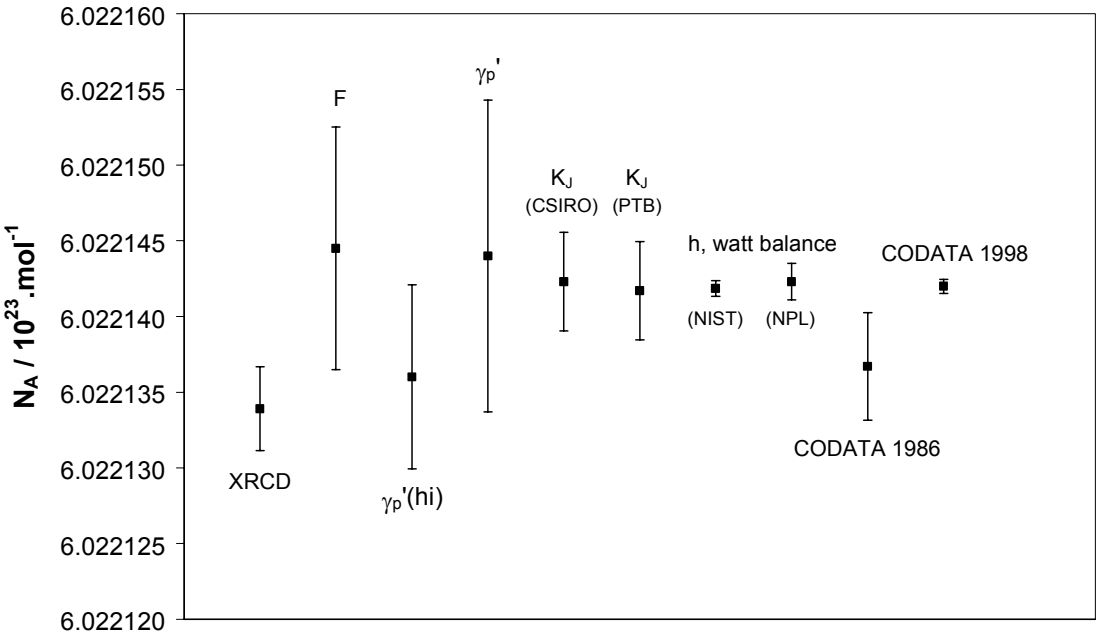

Figure 4 Indirect determinations of the Avogadro number by evaluation of other physical constants.

3.2 Ion accumulation

An alternative method to XRCD for determining the Avogadro constant is ion-accumulation. The ion accumulation experiment involves charged atoms (^{197}Au ions in the case of the latest PTB experiment [18]), being extracted from a gas discharge source in the form of an ion beam which is fired at a collecting target where a mass of up to 10g is accumulated and measured using a quartz microbalance. The number of atoms accumulated is calculated by measuring the ion current and the time this has flowed for, and thus the mass of a gold atom m_{Au} can be determined. Gold ions are accumulated up to a weighable mass m, and the ion current I is integrated over the accumulation time t. With the known charge e of an ion, the mass of a gold atom m_{Au} or the atomic mass unit m_{u}, may be determined using the relative atomic mass of gold A_{Au}. The determination of the Avogadro constant from ion accumulation methods may be described in terms of the amount of substance transmitted on the molecular level to the amount of substance collected on the macroscopic level thus:

$$\frac{i\Delta t}{N_A e} = \frac{m}{RMM} \tag{13}$$

Where i is the current passed for a time t, e is the electronic charge, m is the macroscopic mass of the transferred artefact with relative molecular mass RMM. To be independent from the elementary charge e, the ion current may run through a resistance R with a voltage drop U by comparing R with the Quantum Hall resistance, and U with the Josephson voltage. The atomic mass m_{Au} can thus be traced to the kilogram and second.

Similarly to XRCD methods, ion accumulation has not yet achieved a relative uncertainty of 1 part in 10^8 and needs further input to advance the measurement science in this area. In particular ion accumulation could benefit from new artefacts and materials from which to extrude an ion beam. Such a new material would have the same basic requirements as new artefacts for XRCD but would also require as high a relative molecular weight as possible to minimise the final measurement uncertainty and the counting problem. Very large species could even be counted by more conventional means such as probe microscopy. Ion accumulation currently seems a promising area for Avogadro determination research since the current limiting factor in the final measurement uncertainty is the characterisation and the stability, especially with relation to charge, of the ion beam.

4 New artefacts and materials

The major remaining uncertainties in the determination of N_A via XRCD techniques were discussed in Section 2.3 and arise from the uncertainty in the exact composition and structure of the silicon artefacts [19], i.e. the unknown deviation of the artefact from an ideal silicon single crystal. A possibility for a better determination of N_A would be to find a more suitable artefact for study, with a more rigorously determined composition and structure, or an artefact possessing fewer structural defects and compositional impurities than silicon. The ideal artefact for N_A determination would possess a large mass and be obtainable in a form that is isotopically pure and free from defects and impurities. These are very difficult criteria to meet and improvements in N_A determination are most likely to lie in new experimental methodologies.

If one changes what is being counted during a determination of the Avogadro number, structural and compositional uncertainties may be reduced significantly. For example, if atoms are replaced by molecules or macromolecules we now have entities which are comprised of hundreds, thousand or even millions of atoms and, depending on the particular choice, may have defect levels as low as 1 part in 10^{12}.

The search for new, stable and reproducible artefacts for either ion accumulation or XRCD experiments is of great importance. New artefacts would ideally improve on currently used gold and silicon materials in three major areas:

- *Heavier molecules*
    - Advantage: This leads to more accurate weighing.
    - Problem: Difficult to achieve monodispersivity at high molecular mass.

- *Fewer isotopes*
    - Advantage: This leads to more accurate RMM determination. Monoisotopic materials (such as gold) are ideal.
    - Problem: Becomes more difficult to achieve with large hetero-atomic artefacts. The availability of useable monoisotopic artefacts will decrease with artefact complexity.

- *Improved chemical purity*
    - Advantage: This leads to fewer corrections for impurities.
    - Problem: Large artefacts are more difficult to purify successfully.

Several candidates for suitable artefacts for both XRCD and ion accumulation are reviewed in the following sections.

4.1 Clusters and Fullerenes

Some of the most promising result from the field of cluster chemistry. Work has been carried out on determining the energetics and structure of nickel clusters [20]. These metallic clusters have been shown to form regular single crystal geometric structures. They have also been shown to range in size from 142 to 17000 atoms at which point the onset of optimally stabilised single crystal nickel clusters is estimated to occur. The

very large, very regular structure of these clusters makes them very suitable for Avogadro number experiments. However in terms of XRCD experiments, a 17000 atom artefact is still very small and one needs to be sure that the cluster exists as a single, un-twinned crystal, which is a particular problem for these large clusters. For use in an ion accumulation experiment it would be important to ensure that each cluster carried the same charge in the ion beam upon ionisation.

An alternative to the nickel clusters mentioned above are self-assembled heterogeneous cluster materials [21]. These are usually composed of metals with closed electronic shells and are highly stable. These are good candidates themselves for Avogadro number determination but also represent good candidates as structural templates during the synthesis of novel materials. These clusters are commonly composed of lead and alkali metals (regular tetrahedral lead clusters surrounded by alkali cations), for example Li_4Pb, Li_6Pb, Na_4Pd, Na_6Pb, K_6Pb and K_4Pb. The electronic structure and partial charging on these clusters mean that they less likely to exhibit variable charging and may be suitable for ion-accumulation experiments.

A solution to the problem of twinning and multiple charging in metal clusters is to use cage structures doped with metal atoms. In particular the chemistry of foreign-atom-doped fullerenes offers considerable possibility. Endohedral fullerenes (foreign atoms contained within a $C_{60(\text{or greater})}$ cage), heterofullerenes (where a foreign atom has replaced a carbon atom in a fullerene) are both possible classes of compound that could prove useful in Avogadro determinations. An example of both classes of compound is shown in Figure 5.

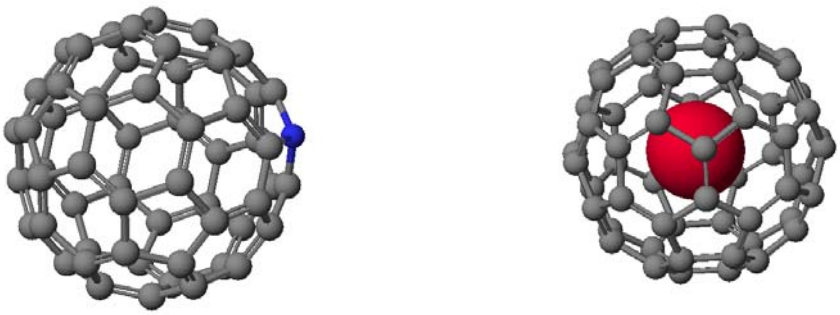

Figure 5 A heterofullerene (left) and an endohedral fullerene (right) from reference 22.

They are relatively simple to synthesise and purify and after purification show almost no structural defects. The presence of a metal atom within the fullerene cage makes it more likely that the doped fullerene unit will carry a consistent charge in an ion beam for the accumulation experiment. The synthesis of $Y^{3+}@C_{82}^{3-}$ and $La^{3+}@C_{82}^{3-}$ (where @ signifies that metals ion is encapsulated within the fullerene structure) has recently been reported [23]. One of the most distinct features of such a metallofullerene is superatom character, by which the metallofullerene can be viewed as a positively charged metal core surrounded by a negativity charged cage. This demonstrates the charge separation characteristics that would be important if such a molecule was used in an ion accumulation experiment. However, some metals, such as sodium, calcium and scandium, are unstable within the fullerene matrix and will destroy the carbon cage. Additionally the fullerene itself will not be isotopically pure and the total molecular

weight of these molecules is relatively low in comparison with the metal super-clusters. However, the synthesis and purification of fullerenes is now very well understood and these would be one of the simplest, most reproducible artefacts to use in Avogadro number determinations. It has been shown that it is also possible to contain nitrogen [24] and noble gas atoms [25] within the fullerene structure.

Endohedral fullerenes containing metal atoms with favourable magnetic properties are particularly attractive artefacts for Avogadro number determination. Heavy transition metal atoms with partially filled 3d, or especially 4f, atomic orbitals would be paramagnetic, potentially with a high spin, and would enable complementary and improved beam steering and detection using external magnetic fields.

An alternative method for the synthesis of endohedral-type fullerenes is by the catalytic growth of carbon nanotubes with vapourised ferromagnetic metals [26]. Using the co-vapourisation of carbon and ferromagnetic metals in an arc generator it is possible to produce very large metallofullerenes and more interestingly, graphite encapsulated nanocrystals of magnetic atoms. The catalytic growth process allows very long nanorods to be grown with very high molecular weights. The results described when cobalt was used for this process are unique. The carbon nanorods in this case were rubbery in texture, unlike the normal crumbly fullerene soots, and were physically and chemically stable and could easily be peeled off the growth chamber walls. There was also extensive crossing linking of the nanotubes resulting in a hyperbranched network of carbon tubes. The soot and nanotube matrix were ferromagnetic. Theoretical calculations predict that the nanotubes may be metallic or semiconducting depending on their pitch. It was also observed that these tubes terminated at spherical fullerene particles which were shown by TEM to contain cobalt nanocrystals of up to 20 nm in size. The nanotubes grown have been shown to be single walled and it may be possible to isolate large quantities of this material. The use of these structures in Avogadro determinations would depend on the ease of separation and purification of the crude material.

Following on from branched nanotubes there have recently been proposals for the synthesis of very high molecular weight dendrimers (hyperbranched molecules with very well defined topology and structure) templated by fullerene molecules. An example of such molecule is shown in Figure 6.

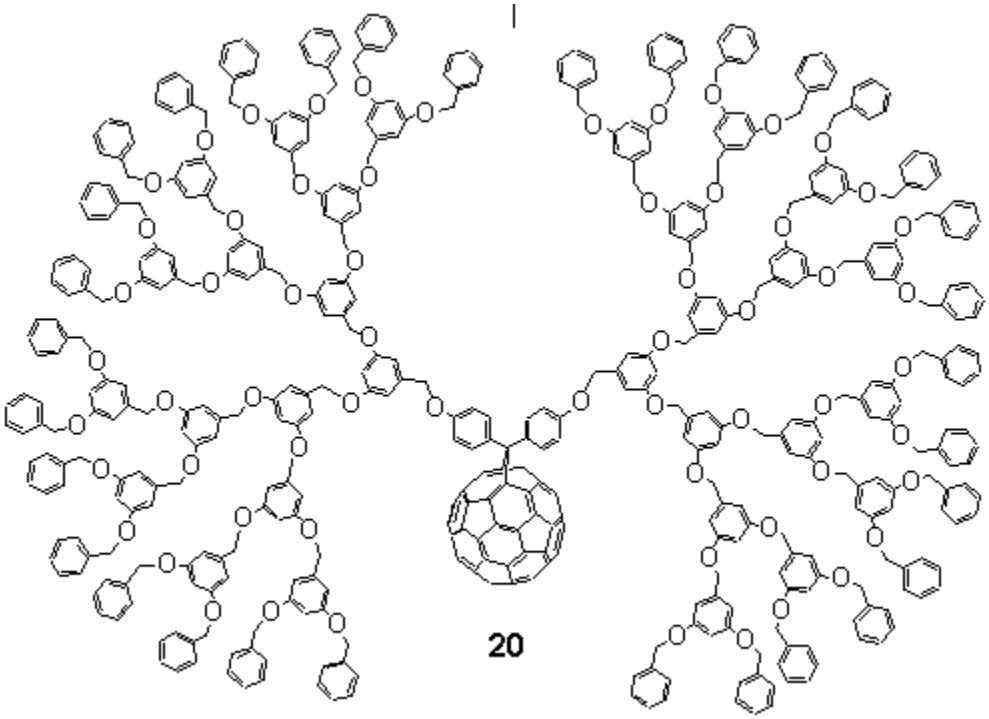

Figure 6 An example of fullerene-templated dendritic structure from reference 27.

Figure 5 represents a fourth generation dendrimer (the dendrimer shell consists of 4 levels) templated in the centre by a fullerene. Dendritic molecules are well-defined macromolecules topologically based on fractals. These highly branched molecules are synthesized from identical building blocks that contain branching sites via a repeatable synthesis strategy. By a judicious choice of these branched building blocks and functional group chemistry, one can precisely control properties of the target molecules such as shape, dimensions, density, polarity, flexibility, and solubility. Dendrimers combine typical characteristics of small organic molecules like defined composition and monodispersivity with those of polymers such as high molecular weight and their resulting multitude of physical properties. A similar combination of characteristics is present in biopolymers like enzymes. Dendrimers consist of one or several cascades attached to a multifunctional central core, which can be an atom, molecule or an ion. The possibility to achieve different addition patterns in a controlled way turns C_{60} into a valuable synthon of unique characteristics to be used as a core. These molecules may even be combined with lipid bilayers to produce even higher molecular weight bio-entities. The dendrimer synthesis route to fullerene chemistry provides readily defined, extremely reproducible, easily synthesised high molecular weight entities. These macromolecules may well prove useful for N_A determinations, especially if the templating fullerene is a metallo-endohedralfullerene.

Silicon is also a useful material in cage and cluster chemistry. Recent computational studies have speculated upon the existence of large silicon cluster containing up to 45 atoms. These clusters have been shown to have completely different properties from bulk silicon and clusters containing above 36 atoms for a fullerene-like cage structure in which it may be possible to encapsulate heavy metal atoms [28]. These structures would be interesting targets for Avogadro determinations but first their existence, stability and ease of purification would have to be proved experimentally before they

could seriously be considered for use. Smaller, less regular silicon cage clusters capable of encapsulating metal particles have recently been reported [29]. In this case, reaction of silane with transition metal ions has produced dehydrogenated MSi_n^+ cluster ions where n has been observed to be as high as 14. The central metal ion is of great importance since the small silicon cage is unstable without a stabilising ion. This study has confirmed for the first time that, the metal ion is actually encased within the silicon cage. For specific compositions the silicon cages remain dehydrogenated, suggesting that they are so stable that they could be used as tuneable building blocks for cluster-assembled materials. This property may be particularly valuable in the fabrication of high, but consistent molecular weight artefacts.

Another metal trapping molecule which offers possibilities in the field of Avogadro number determination is the calixarene (or 'Greek urn') family of molecules [30,31]. These molecules are now commonly used in analytical chemistry to detect and trap and detect heavy metals in liquid waste streams [32]. Calixarenes coordinate particularly strongly to transition metal ions and can form complexes of regular and very high molecular mass (over 1000 mass units). These molecules are easily synthesised and purified, even after coordination to a metal. Calixarenes are also being used in metal speciation studies. An example of a calixarene molecule is show in Figure 7.

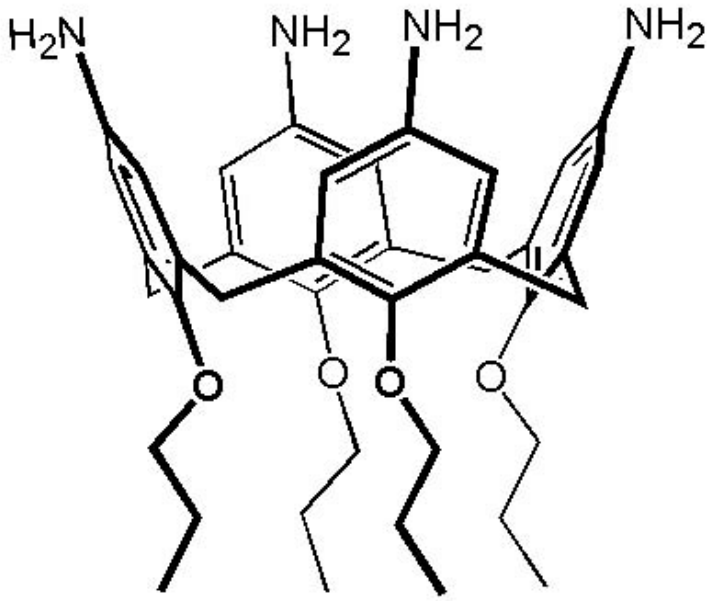

Figure 7 A molecule from the calixarene family (from reference 33).
Metal ions would coordinate in the top, 'cup-like' portion of the molecule.

4.2 Macromolecules

Recently, research into the formation of nanostructures aimed at forming active parts of MEMS or NEMS devices has resulted in the construction of hybrid organic molecule/silicon devices [34]. Styrene has been polymerised on highly ordered, H-terminated silicon surfaces to form well defined polystyrene wires of very high but

accurately known and controlled molecular weight. This self-directed growth of molecular-based nanostructures on silicon may prove sufficiently controllable to be a useable high-mass artefact for ion accumulation work. Along similar lines the doping of Europium ions in Y_2O_3 nano-crystals [35] offers possibilities for well-defined, high molecular weight, singly charged artefacts for XRCD and ion accumulation study.

A potentially suitable artefact closely related to both the existing ion accumulation technology and fullerene/cluster chemistry is the recently reported fullerene-functionalised gold nanoparticles [36]. A self-assembled photoactive antenna system containing a gold nanoparticle as the central nanocore and appended fullerene moieties as the photoreceptive hydrophobic shell has been designed by functionalising a gold nanoparticle with a thiol derivative of fullerene. Upon suspension of fullerene-functionalized gold nanoparticles (Au-S-C_{60}) in toluene, 5-30 nm diameter clusters were observed. These nanoparticles have high molecular weight and a stable, structurally regular fullerene core but the variability in chemistry and size within a batch of nanoparticles would mean that either further preparative or separation science would need to be employed before these entities were suitable for N_A determination.

Electrochemistry on the nanoscale has also been used as a fabrication method for metallic clusters [37]. By employing a special scanning tunnelling microscope called an "electrochemical STM" the STM's needle like probe was immersed at the gold surface under study in an electrolyte consisting of copper sulphate and sulphuric acid. The STM's electrically conducting needle and the metallic gold surface acted like two electrodes in the set-up. Then 60-nanosecond-length voltage pulses between the needle and the gold surface were applied, resulting in surface pits with 5 nm diameter and depths of 0.3-1 nm. It is believed that the voltage pulse oxidized the gold creating gold ions which were then attracted to the tip, where they were reduced. Reversing the voltage, 1 nm high, 8 nm diameter clusters of copper were deposited (formed by the reduction of copper ions from the electrolyte). The ultra-short pulses allow the electrochemical changes to be made on an extremely localised level. The size of the clusters produced is also controlled by the magnitude of the reverse current that is passed.

The recent discovery of superconducting balls has lead to particles with a similar shape to fullerenes and metal nanoclusters but on a much larger scale [38]. Micron-sized copper oxide (e.g., Br-Sr-Ca-Cu-O) superconducting particles (suspended in liquid nitrogen) in an electric field running between two electrodes were observed to self-assemble themselves into a ball. The ball, about 0.25 mm across and containing over a million particles (shown in Figure 8), formed quickly under the experimental conditions and was quite robust. Artefacts on this scale are very promising for several types of experimental Avogadro number determination but the superconducting ball technology would first need to be refined to produce particles which were of a consistent mass and exhibited a more regular structure and shape (especially for XRCD type determinations).

Figure 8 Scanning electron micrograph of a 0.25-mm-diameter ball consisting of Bi-Sr-Ca-Cu-O particles packed closely together. From reference 39.

As shown in the example of the superconducting balls, above, a desirable form of nanocrystal structure is self-assembly. If nanocrystals can self-assemble into a macro crystalline material then the production of artefacts for N_A determination with very low defect levels may be possible. Work involving the self-assembly of nanocrystals around adsorbed thiolate groups has recently been reported [40]. Self-assembly of nanocrystals involves organization of nanocrystals encapsulated by protective compact organic molecules into a crystalline material. The adsorbed molecules not only serve as the protection layer for the nanocrystals but also provide the dominant cohesive interactions sustaining the nanocrystal superlattices. The length of the adsorbed molecules, in this case the thiol, is a controllable parameter, making the ratio of particle size to inter-particle distance an adjustable parameter that sensitively tunes the inter-particle interaction and resulting collective properties. Bundled and interdigitated thiolate molecules have been adsorbed on Ag nanocrystals and have been observed using energy-filtered transmission electron microscopy. In these orientationally ordered, self-assembled Ag-nanocrystal superlattices, the bundling of the adsorbed molecules on the nanocrystal surfaces is the fundamental structural motif and can be repeated exactly on a large scale to produce very high mass collections of Ag nanocrystals bound together by thiolate layers. Such structures also show very low defect levels over hundreds of nanometers.

A complementary method for the templating and growth of nano-sized particles is the use of colloidal assemblies and liquid crystal based systems [41]. Such a technique aims to fabricate an assembly of perfect nanometer-scale crystallites (quantum crystals) identically replicated in unlimited quantities in such a state that they can be manipulated and understood as pure macromolecular substances. Several approaches have been used to create 3D structures in this way. Inorganic-organic superlattices have been synthesised using multiplayer cast films [42]. By a combined synthesis procedure in reverse micelles with the precipitation of complementary materials, highly ordered nano-composites are formed [43]. Another approach to obtaining 3D structures is to

assemble the nanoparticles in ordered arrays. This requires only a hard sphere repulsion, a controlled size distribution and the inherent van der Waals attraction between particles and dispersion forces. Polydispersivity of the nano-particles prevents the construction of well-defined structures. Under these circumstance electrodeposition [44] and Langmuir-Blodgett [45] techniques can help favour regular structure formation. Recently, colloidal self-organisation of nanocrystallites has been observed for metal and semiconductor particles surface passivated with coordinating ligands such as alkanethiols [46], alkylphosphines [47] and dithiols [48].

4.3 Biological structures

A less conventional arena to search for new artefacts for the Avogadro number determination is the biotechnological area and the potential use of biological molecules and even biological entities. An interesting example of a biological entity representing a suitable high mass artefact is the bacteriophage virus, shown in Figure 9.

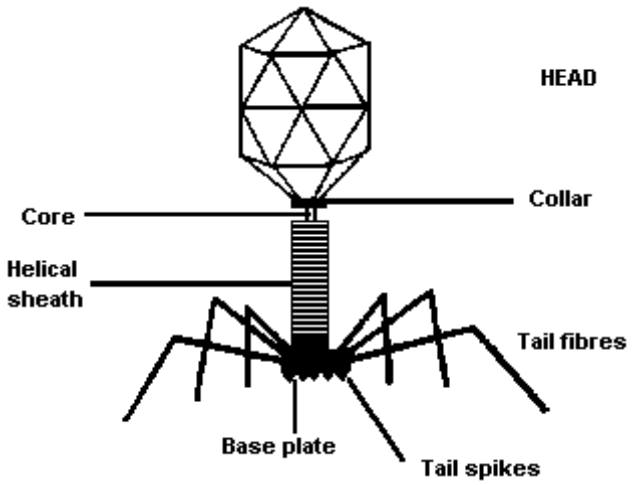

Figure 9 A T-even bacteriophage. From reference 49.

Viruses straddle the definition of life. They lie somewhere between supra molecular complexes and very simple biological entities. Viruses contain some of the structures and exhibit some of the activities that are common to organic life, but they are missing many of the others. In general, viruses are entirely composed of a single strand of genetic information encased within a protein capsule. A bacteriophage is a virus which infects bacteria. In particular, the bacteriophage T4 is a virus that infects E.Coli, a bacteria that has been used extensively for molecular biology research. The bacteriophage T4 exemplifies the life cycle of viruses. It exists as an inactive virion until one of its extended 'legs' comes into contact with the surface of an E. Coli. Sensors on the ends of its 'legs' recognize binding sites on the surface of the host's cell, and this triggers the bacteriophage into action. The bacteriophage binds to the surface of the host, punctures the cell with its injection tube, and then injects its own genetic blueprint. In nature, the bacteriophage T4 contains about 168,800 base pairs of double stranded DNA. This genetic blueprint contains all of the necessary information to create new bacteriophage T4.

One bacteriophage may have a mass of 9 ng and, more importantly only exhibits very low defect levels for a biological entity. Additionally, in terms of Avogadro number determinations, bacteriophages, and biologicals of this magnitude in general, may be counted using more traditional, scanning probe, or optical microscopy techniques. These viruses thus provide 'particles' of 10^7 mass units (compared to 197 mass units for a gold atom) and hence reduce the counting problem by 6 orders of magnitude.

The observation of DNA membrane self-assembly offers the possibility of extremely high mass self-assembled biological materials with very little mass variation [50]. Such a material has been formed by the mixing of negatively charged DNA molecules with positively charged artificial versions of the membranes that form the protective coverings of cells. These complexes are presently used as delivery vehicles in gene therapy and have a highly organised internal structure. Again the mass of such a moiety may be as high as 10^7-10^8 mass unit, hence reducing counting problems.

Rotating bacteria which have been observed, not only to rotate themselves, but also to move together in a single direction like a flock of birds, provide the possibility of high mass biological artefacts with additional regular shape and structure [51]. In this case the regular shape and structure is a result of the bacteria's rotation. An image of rotating bacteria is shown in Figure 10.

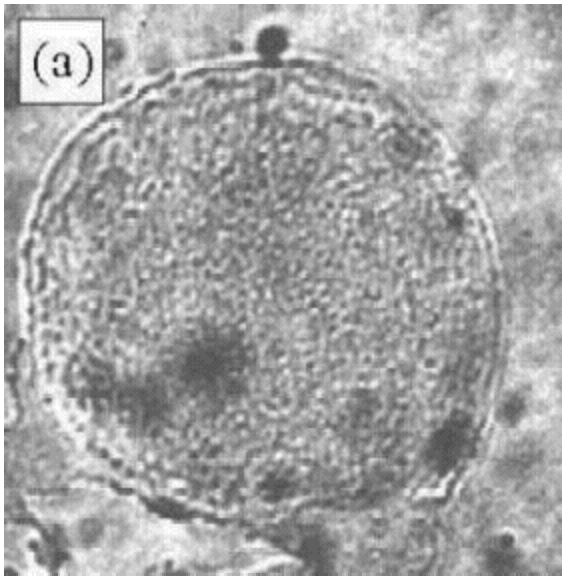

Figure 10 Still image of a rotating group of bacteria (B. subtilis) with a magnification of 500 times original size. From reference 52.

Proteins represent another biological entity, which has the potential to be a new type of artefact for Avogadro constant determination. Whilst DNA is responsible for the storage of genetic information, it is proteins that maintain and reproduce DNA, as well as carrying out metabolic and structural functions to keep cells alive. Proteins are formed from complex combinations of many amino acid residues. There are 20 naturally occurring amino acids used in proteins. An individual protein's structure and operation is very well defined as required by the specific biological process it regulates. Hence proteins have very high and very well defined masses with low defect rates and low mass variability, all suitable qualities for Avogadro artefacts.

Further protein-related biological artefacts that the potential for used in Avogadro constant determination are self-assembly DNA. A diagram of a DNA self-assembly is shown in Figure 11. These very large are formed by mixing DNA molecules with artificial versions of the membranes that form the protective coverings of cells, are highly organized at length scales from nanometers to microns. These materials, currently serving as gene delivery vehicles, are made of layers consisting of rows of equally spaced, single DNA molecules alternating with sheets of membrane. The self-assemblies molecules in these materials are aligned over length scales of microns. The spaces between molecules form organized arrays of "nanopores" which have many possible chemical applications. In addition, these materials can potentially serve as templates for the fabrication of inorganic nanostructures with geometries and features that were previously impossible to achieve. DNA self-assemblies have very high molecular masses (up to 10^{10} amu) which could prove useful for Avogadro number determinations relying on more conventional counting techniques such as scanning probe microscopy. However the structures would be relatively difficult to purify and would show considerable mass variability.

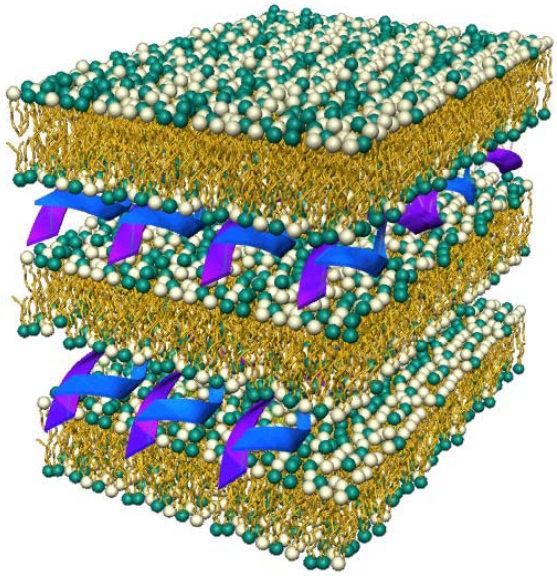

Figure 11. Diagram of a DNA-membrane complex, a material formed by mixing negatively charged DNA molecules with positively charged artificial versions of the membranes that form the protective coverings of cells. The purple and blue ribbons represent the DNA double helices, which form a one-dimensional lattice between a double-layer sheet of the membrane. The green and white spheres represent the hydrophilic ("water-loving") ends of the charged and neutral molecules that respectively make up the membrane. The yellow chains (two to each sphere) represent the hydrophobic ("water-fearing") hydrocarbon "tails" in the molecules. From reference 53.

A summary of the characteristics and suitability of the ‘large molecule’ artefacts discussed in the sections above is given in Table 2.

Artefact Type	Approximate mass	Mass Accuracy	Purification	Suitability
Small molecular Ni clusters	10^4-10^6 amu	Low	Easy	Difficult to achieve single ionisation
Lead centred clusters	450 amu	Very high	Easy	Easy to achieve consistent single ionisation, but very low mass
Silicon cages	300+ amu	High	Intermediate	May shown some instability
Endohedral-fullerenes	1000 amu	High	Easy	Easy to achieve consistent single ionisation. Relatively low mass
Hetero-fullerenes	1000-1500 amu	High	Easy	Easy to achieve consistent single ionisation. Relatively low mass
Templated dendrimers	10^3-10^4 amu	Intermediate	Difficult	Large mass. Central metal would assist consistent ionisation
Metallo-Calixarenes	800+ amu	Very high	Intermediate	Suitable for ionisation with careful choice of bound metal atom
Fullerene-Au nanoparticles	10^6+ amu	Low	Difficult	Multiple ionisation a problem
Superconducting balls	10^9+ amu	Low	Difficult	Suitable high mass, but purification a problem
Liquid crystal templated nanoparticles	10^7+ amu	High	Intermediate	Multiple ionisation a problem
Proteins	10^3-10^6 amu	Very High	Easy	Consistent ionisation may be a problem
Bacteriophage virus	10^7 amu	Very high	Easy	Defects / ionisation may be a problem
Rotating bacteria	10^7 amu	High	Difficult	Biological purification a problem
Self-assembly DNA	10^7-10^9+ amu	Intermediate	Intermediate	Mass variability is a problem

Table 2. Characteristics and suitability of the 'large molecule' artefacts discussed in Section 4.

5. New technologies for N_A measurement with large molecules

Table 2 suggests that hetero- and endohedral-fullerenes and proteins are the most promising new artefacts for use in the determination of the Avogadro constant. A review of new technologies for N_A determination needs therefore to consider primarily the experimental use of these artefacts.

5.1 High current ion guns

C_{60} ion guns are now commercially available [54] and there seems no reason why the principle used in these instruments cannot be adapted to produce ion beams from the artefacts listed above for ion accumulation experiments. C_{60} ions are produced in the IOG C_{60} instrument by electron bombardment. A small charge of C_{60} powder at the rear of the source is heated to produce C_{60} vapour. This vapour passes into the centre of an electron bombardment chamber. The C_{60} ions and other positively charged fragments, are extracted, and accelerated to full voltage as they enter the optical column. The IOG C_{60} optical column has two lenses, the first forming a field image approximately halfway down the column, the second forming the final probe. Beam pulsing is done by a pair of short plates positioned at the intermediate field image. Mass filtering is achieved by chopping between different mass-pulses at a second pair of pulsing plates further down the column. Sputter yields at different filter settings indicate that around two thirds of ions in the beam are C_{60}^{+}. The column also contains provision for pulse bunching, beam rastering, alignment and stigmation. A 1° bend in the axis serves to reject neutrals from the beam. The optics are enclosed in a vacuum assembly which includes a steering bellows for accurate positioning of the gun, a gate valve for isolation of the source chamber and a port for differential pumping. The gun is suitable for use on UHV chambers and is bakeable to 150°C so it would be possible to perform experiments using a variety of different artefacts without contamination problems.

The present deficiency of the C_{60} ion gun is that the ion current produced is only 10 nA and hence ion accumulation experiments which produced an accurately weighable mass of C_{60} would prove extremely lengthy. However, technology in this area continues to advance and ion currents are continually increasing.

Nano-cluster ion sources are still at an early stage of development but the first commercial example has recently been launched using gas condensation technology [55]. Using either magnetron sputtering or simple evaporation almost any material can be induced to form clusters as it is maintained in a high-pressure, ultra-cold gaseous environment. The clusters then pass through an aperture and a gas skimmer into the growth chamber. Here the clusters are deposited onto the substrate with negligible kinetic energy to allow retention of the crystalline properties. In the case of magnetron-generated material, a substantial fraction of the clusters are negatively charged, thus permitting their manipulation by electric fields. By varying the cluster path-length, their size can be broadly pre-determined in the clustering chamber.

5.2 Ion-cyclotron resonance mass spectrometry

The use of high mass artefacts in ion accumulation techniques may mean that more advanced equipment is needed to collect, separate and detect these particles. A candidate technology for this purpose is Ion-Cyclotron-Resonance Mass Spectrometry (ICR-MS). ICR-MS is a technique in which ions are subjected to a simultaneous radio frequency electric field and a uniform magnetic field, causing them to follow spiral paths in an analyser chamber. By scanning the radio frequency or magnetic field, the ions can be detected sequentially. Detailed descriptions of ICR-MS theory are available [56].

ICR MS was brought to the attention of chemists in the middle to late 1960s and has been used extensively in the field of ion-molecule reaction characterisation.

In 1974 ICR was revolutionised by the development of Fourier transform ICR mass spectrometry (FT-ICR MS). The major advantage of FT-ICR MS is that it allows many different ions to be determined at once, instead of one at a time. The technique is also known for its mass resolution, which is higher than that of any other type of mass spectrometer. A resolving power of $>10^5$ and mass accuracy of <1ppm are routinely achieved. Most importantly this technique is also able to measure and resolve very high mass artefacts and would be most useful in ion-accumulation experiments for N_A determination. For example, multiply-charged molecular ions of large biomolecules (proteins, DNAs, polysaccharides etc) with molecular masses up to several million mass units, or Daltons, can be stored, manipulated and analysed inside the cell of a Fourier transform ion cyclotron resonance mass spectrometer [57] using electrospray ionisation (ESI) [58] or matrix-assisted laser desorption ionisation (MALDI) [59] techniques. FT-ICR-MS has the potential to remove the mass variability from very large mass artefacts using the technique's high mass resolution and high mass capability.

5.3 SQUID ion current detectors

Superconducting quantum interference devices, or SQUIDs, represent another advancing technology that could prove useful in future determinations of the Avogadro constant with ion accumulation techniques. In 1986 a new class of superconducting, ceramic materials was discovered. These materials behave like metals at room temperature, but when cooled down in liquid nitrogen to a temperature of -196°C, they lose their electrical resistance and become superconducting. Due to the relatively high temperature of -196°C, compared to the usual -269°C for the classic superconductors, these materials are called "high-temperature superconductors" (HTS). Of particular interest is the Josephson effect. When two superconducting samples are brought into close contact, such that their macroscopic wave functions overlap, electronic interference effects can be observed. This interference of the macroscopic wave functions of the superconductors can be used to detect and measure local magnetic fields with extremely high sensitivity (sufficient to detect magnetic inclusions in individual cells).

To fabricate superconducting quantum interference devices (SQUIDs) from the HTS materials a thin-film technology has been developed. The ceramic material is

evaporated in an oxygen atmosphere of low pressure and deposited on a substrate material, where it grows in single-crystalline form. These very smooth films are patterned in a multilayer process to form SQUID-magnetometers incorporating two Josephson-junctions.

It is proposed that SQUIDs would be useful counting aids in ion accumulation experiments. The SQUID could be used to measure the tiny currents induced by the passage of each individual ion. Measurements of the ion current of individual ions has been achieved for the accurate determination of atomic masses [60, 61]. Currently, though, the SQUID can only detect the presence of a single ion and not the passage of a moving ion. Predicted maximum count rates of 1000 Hz would also currently be too low for practical use, although technology continues to advance in this area. At present measurements of current in charged particle beams, such as those used in mass spectrometry, have to be measured invasively. Accurate on-line measurement of ion beam currents would be of great use in verifying quantitative mass spectrometry measurements and provide more accurate process control possibilities in the semiconductor industry. NPL, in collaboration with Strathclyde University, has produced a High Temperature Superconductor Superconducting Quantum Interference Device current comparator which can measure charged particle beams non-invasively to an accuracy of better than 0.1% [62]. Measurements are in the range 1nA to 1mA. The ion beam, which can be maintained at ambient temperature, passes through a liquid-nitrogen-cooled superconducting tube. Due to a fundamental property of superconductors (the Meissner effect [63]) a current that is equal but opposite to that of the beam is set up on the outside of the tube. This current distribution is highly insensitive to the position or spatial distribution of the beam within the tube. The external magnetic field set up by the current is measured by a SQUID that indicates the total beam current with very high accuracy. Further work on the HTS SQUID will attempt to increase the sensitivity of the system - extending the range down to pA (10^{-12} A) and experiments will examine methods to servo the beam current to maintain it constant to better than ±0.1%. This technique also offers a possibility of direct measurement of the Faraday fundamental constant and from there a possible direct determination of the Avogadro number. An AFM image of a SQUID is shown in Figure 12.

Figure 12 AFM image of DC SQUID with 2.5 μm hole, showing central hole, Josephson junctions and resistive shunts. From reference 64.

5.4 Improving collection efficiency

The collection efficiency of detectors is of primary importance in ion accumulation and molecular collection experiments. Collection efficiency represents the ratio of the

number of particles registered by the detector to the number of particles emitted by the source. Collection efficiency varies greatly between collection systems and depends critically on the conditions of collection. For example, the collection efficiency of multichannel plate collectors used for the detection of cationised oligomers is known to drop from 80% to 5% as the impact energy decreases from 20 to 5 keV [65]. Low or uncertain collection efficiencies lead to difficult, lengthy and inaccurate ion accumulation experiments. Therefore it is desirable to maximise and accurately evaluate detector collection efficiency. Advances in technology in this area would especially benefit ion accumulation experiments for Avogadro number determination. There are two main types of collector currently used for ion detection.

Channel electron multipliers (CEMs) are detectors, which respond to charged particles, hard and soft X-rays, and ultraviolet radiation. Through the process of secondary electron emission a CEM is capable of detecting a particle or photon that has entered its funnel-shaped input aperture. These primary particles generate secondary electrons that are accelerated down the channel by a positive bias. Upon striking the interior surface of the channel walls these electrons then generate further secondary electrons. The resulting avalanche process produces an easily detectable output pulse of charge containing up to 10^8 electrons with a duration (FWHM) of about 10 nanoseconds. The efficiency of the collecting horn and Faraday cup represents the greatest contribution to overall efficiency [66]. Quite often small patches of higher than average efficiency can be observed within a collecting horn and should be avoided by defocusing the ions to cover the entire detector surface. Currently technological improvements in efficiency focus around better Faraday cup designs and fabrication techniques [67]. A CEM responds to a variety of stimuli in various degrees. The absolute efficiency of a given CEM to a specified input will depend on the surface cleanliness of the CEM, any pre-acceleration potentials that may exist, and the energy and mass characteristics of the input.

A multichannel plate detector (MCPs) is a specially fabricated plate that amplifies electron signals similar to secondary electron multiplier. A MCP has several million independent channels and each channel works as an independent electron multiplier. A MCP consists of a two-dimensional periodic array of very-small diameter glass capillaries (channels) fused together and sliced in a thin plate. A single incident particle (ion, electron, photon *etc*) enters a channel and emits an electron from the channel wall. Secondary electrons are accelerated by an electric field developed by a voltage applied across the both ends of the MCP. These secondary electrons travel along parabolic trajectories until they in turn strike the channel surface, thus producing more secondary electrons. This process is repeated many times along the channel; as a result, this cascade process yields a cloud of several thousand electrons, which emerge from the rear of the plate. If two or more MCPs are operated in series, a single input event will generate a pulse of 10^8 or more electrons at the output. Performance and efficiency may be improved by stacking multiple MCPs on top of one another. Two common forms are the multiple MCP chevron and Z-stack design. The chevron design consists of just two MCP wafers stacked onto each other with opposing tilt directions. The shower of electrons from one MCP will enter the pore of the other at an angle, improving efficiency. For low-energy impacys onto the detector the spread in efficiency may be as much as 100% of the mean efficiency. This effect reduces as the energy of ion impacts increases.

Novel detectors are being developed in an attempt to improve collection efficiency, for example, detection schemes that rely on heat pulse detection where the kinetic energy of impacting ions is converted into heat when ions strike a detector [68]. However, these detectors are still in the early stages of development. Other advances in detector design include the use of new, longer lifetime, more specialised materials on dynode surfaces to increase secondary electron emission, improve gain and increase efficiency.

6. Summary

The Avogadro number, N_A, is the scaling factor between the macroscopic and atomic worlds. It allows one to see quantity in the macroscopic world as being a multiple of a quantity on the atomic scale.

- The eventual goal of N_A measurement is to obtain determinations which have a relative uncertainty of 1 part in 10^8 or less. At this stage measurement of N_A would represent a definition of mass superior to the kilogram artefact at BIPM.

- Current methods for the measurement of the Avogadro constant, such as X-ray crystal density determinations of highly pure silicon artefacts, quote measurement uncertainties, which are an order of magnitude greater than the critical level. Even with advances in the measurement of the structure, defect concentration and in particular, the isotopic ratio of silicon artefacts [69], it seems unlikely that determination of N_A will replace the kilogram artefact within the near future without recourse to new experimental methods and novel chemical artefacts.

- Advances in structural and synthetic chemistry mean that, ion accumulation methodology has a wide selection of possible high mass, low defect artefacts available to it. In particular metallo-endohedral fullerenes seem to represent extremely promising high mass artefacts.

- The advent of new ion beam sources and the use of SQUIDs for low level, high accuracy, ion current detection adds further experimental potential to the ion accumulation method.

7. Acknowledgements

The authors would like to thank John Gallop and Jeff Flowers for useful discussions during the preparation and review of this report.

8. References

1 M. J. T. Milton and T. J. Quinn, *Metrologia*, 2001, **38**, 289.
2 P. De Bievre, S. Valkiers and P. D. P. Taylor, *Fren. J. Anal. Chem*., 1998, **361**, 227.
3 http://physics.nist.gov/cgi-bin/cuu/Value?na
4 P. Becker, *Rep. Prog. Phys*., 2001, **64**, 1945.
5 T. J. Quinn, *IEEE Trans. Instrum. Meas*., 1991, **40**, 81.
6 S. I. Salem, T. Boughter-Cardin, M. T. Civalleri, J. W. Leonard and G. A. Williams, *Am. J. Phys*., 1988, **56**, 466.
7 http://dekalb.dc.peachnet.edu/~mkim/avogadro.htm
8 V. E. Bower and R. S. Davis, *J. Res. Natl. Bur. Stand*., 1980, **85**, 175.
9 L. J. Powell, T. J. Murphy and J. W. Gramlich, *J. Res. Natl. Bur. Stand*., 1982, **87**, 9.
10 R. T. Birge, *Am. J. Phys*., 1945, **13**, 63.
11 M. E. Straumanis, *Acta Cryst*., 1949, **2**, 84.
12 http://physics.nist.gov/Divisions/Div842/Gp5/crystalc.html
13 http://www.npl.co.uk/mass/avogadro.html
14 A. Ulyashin, R. Job, W. Fahrner, A. Mudryi, A. Patuk and I Sakin, *High Purity Silicon VI SPIE*, ed C. I. Claeys, 2000, **4218**, 66.
15 P. Becker, H. Bettin, P. De Bievre, C. Holm, U. Kuetgens, F. Spieweck, J. Stumpel, S. Valkiers and W. Zulehner, *IEEE Trans. Instrum. Meas*., 1995, **44**, 522.
16 P. Seyfried, P. Becker, A. Kozdon, F. Ludicke, J. Stumpel, H. Wagenbreth, D. Windisch and P. DeBievre, *Z. Phys. B. Cond. Matt*., 1992, **87**, 289.
17 B. N. Taylor, *Metrologia*, 1994, **31**, 181.
18 http://www.ptb.de/en/org/1/11/111/ionenex.htm
19 J. Martin, H. Bettin, U. Kuetgens, D. Schiel and P. Becker, *IEEE Trans. Instrum. Meas*., 1999, **48**, 216.
20 C. L. Cleveland and U. Landman, *J. Chem. Phys*., 1991, **94**, 7376.
21 J. A. Alonso, M. J. Lopez, L. M. Molina, F. Duque and A. Mananes, *Nanotechnology*, 2002, **13**, 253.
22 http://www.ifw-dresden.de/iff/11/spec/fulprop/highlights/highlights.htm
23 H. Shinohara, *Rep. Prog. Phys*., 2000, **63**, 843.
24 http://www.nmrc.ie
25 Clusters and Nanomaterials, Eds. Y. Kawazoe, T. Kondow and K. Ohno, Springer, Berlin, 2002.
26 D. S. Bethune, C. H. Kiang, M. S. de Vries, G. Gorman, R. Savoy, J. Vazquez and R. Beyers, *Nature*, 1993, **363**, 605.
27 http://www2.chemie.uni-erlangen.de/services/dissonline/data/dissertation/Francesc_Camprubi/html/chapter3-1a.html#TopOfPage
28 U. Rothlisberger, W. Andreoni and M. Parrinello, *Phys. Rev. Lett*., 1994, **72**, 665.
29 H. Hiura, T. Miyazaki and T. Kanayama, *Phys. Rev. Lett*., 2001, **86**, 1733.
30 R. Ludwig, *Fren. J. Anal. Chem*., 2000, **367**, 103.
31 D. M. Roundhill, *Prog. Inorg. Chem*., 1995, **43**, 533.
32 A. Casnati, S. Barboso, H. Rouquette, M. J. Schwing-Weill, F. Arnaud-Neu, J. F. Dozol and R. Ungaro, *J. Am. Chem. Soc*., 2001, **123**, 12182.
33 http://www.organik.uni-erlangen.de/hirsch/cali_chem.html
34 G. P. Lopinski, D. D. M. Wayner and R. A. Wolkow, *Nature*, 2000, **406**, 48.
35 D. S. Burgess, *Photonics Spectra*, 2000, **October,** 30.

36 P. K. Sudeep, K. George Thomas, M.V. George, S. Barazzouk, S. Hotchandani. and P.V. Kamat, *Nano. Lett*., 2002, **2**, 29.
37 R. Schuster, V. Kirchner, X.H. Xia, A.M. Bittner and G. Ertl, *Phys. Rev. Lett.*, 1998, **80**, 5599.
38 R. Tao, X. Zhang, X. Tang and P. W. Anderson, *Phys. Rev. Lett*., 1999, **83**, 5575.
39 http://www.aip.org/physnews/graphics/html/superball.html
40 Z. L. Wang, S. A. Harfenist, R. L. Whetten, J. Bentley and N. D. Evans, *J. Phys. Chem. B*, 1998, **102**, 3068.
41 M. P. Pileni, *Langmuir*, 1997, **13**, 3266.
42 N. Kimizuka and T. Kunitake, *Adv. Mater*., 1996, **8**, 89.
43 S. Y. Chang, L. Liu and S. A. Asher, *J. Am Chem. Soc*., 1994, **116**, 6739.
44 M. Giersig and P. Mulvaney, *Langmuir*, 1993, **9**, 3408.
45 J. H. Fendler and F. Meldrum, *Adv. Mater*., 1995, **7**, 607.
46 P. C. Ohara, D. V. Leff, J. R. Heath and W. M. Gelbart, *Phys. Rev. Lett*., 1995, **75**, 3466.
47 C. B. Murray, C. R. Kagan and M. G. Bawendi, *Science*, 1995, **271**, 1335.
48 M. Brust, D. Bethell, D. J. Schiffin and C. J. Kiely, *Adv. Mater*., 1995, **9**, 797.
49 http://www.bmb.leeds.ac.uk/mbiology/ug/ugteach/icu8/introduction/viruses.html
50 J. O. Rädler, I. Koltover, T. Salditt, and C. R. Safinya, *Science*, 1997, **275**, 810.
51 A. Czirok, E. Ben-Jacob, I. Cohen, O. Shochet and T. Vicsek, *Physical Review E*, 1996, **54** , 1791.
52 http://www.aip.org/physnews/graphics/html/bacteria.htm
53 http://www.aip.org/physnews/graphics/html/dna_memb.htm
54 http://www.ionoptika.com/details.htm
55 http://www.tectra.de/news.html#Gas%20Condensation%20Nano-Cluster
56 http://www.ionspec.com/tutorial.html
57 G. J. Feistner, K. F. Faull, D. F. Barofsky and P. Roepstroff, *J. Mass Spec*., 1995, **30**, 519.
58 J. B. Fenn, M. Mann, C. K. Meng, S. F. Wong and C. M. Whitehouse, *Science,* 1989**, 246***,* 64.
59 M. Karas, U. Bahr and F. Hillenkamp, *Int. J. Mass Spectrom. Ion Processes*, 1989*,* **92**, 231.
60 http://rleweb.mit.edu/Publications/pr143/chapter-16a-web.pdf
61 R. Weisskoff, *J. Applied Physics*, 1988, **65**, 4599.
62 http://www.npl.co.uk/annualreview/1999/14ther_a.html
63 http://www.chem.ox.ac.uk/vrchemistry/super/meissner.html
64 http://www.npl.co.uk/npl/cbtm/bmg/stm/vtuhvstm_projects_sqd.html
65 I. S. Gilmore and M. P. Seah, *Int. J. Mass Spec*., 2000, **202**, 217.
66 I. S. Gilmore and M. P. Seah, *Applied Surface Science*, 1999, **144**, 113.
67 I. S. Gilmore and M. P Seah, *Surf. Inf. Anal*., 1995, **23**, 248.
68 http://www.ornl.gov/hgmis/publicat/96santa/sequenci/benner.html
69 P. De Bievre, S. Valkiers, H. S. Peiser, P. Becker and J. Stumpel, *IEEE Trans. Instr. Meas*., 1995, **40**, 530.